p.50

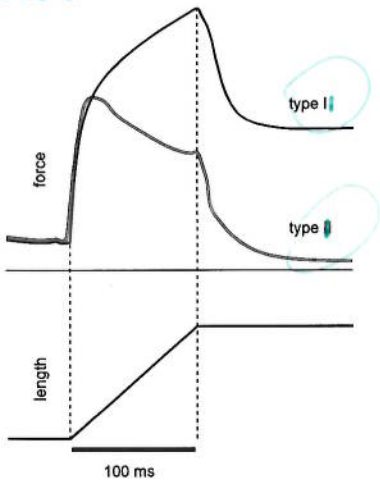

Figure 3.8

p.61

$$K = \frac{d\tau}{dq} = \frac{d(\tau_+ - \tau_-)}{dq} = \frac{\rho_+ d\mu_+}{dq} - \frac{\rho_- d\mu_-}{dq} = \frac{\rho_+ d\mu_+}{d\lambda_+/\rho_+} - \frac{\rho_- d\mu_-}{-d\lambda_-/\rho_-}$$
$$= \frac{{\rho_+}^2 d\mu_+}{d\lambda_+} - \frac{{\rho_-}^2 d\mu_-}{-d\lambda_-} = {\rho_+}^2 K_{\mu+} + {\rho_-}^2 K_{\mu-} \qquad (4.5)$$

$$D = \frac{d\tau}{d\dot{q}} = \frac{d(\tau_+ - \tau_-)}{d\dot{q}} = \frac{\rho_+ d\mu_+}{d\dot{q}} - \frac{\rho_- d\mu_-}{d\dot{q}} = \frac{\rho_+ d\mu_+}{d\dot{\lambda}_+/\rho_+} - \frac{\rho_- d\mu_-}{-d\dot{\lambda}_-/\rho_-}$$
$$= \frac{{\rho_+}^2 d\mu_+}{d\dot{\lambda}_+} - \frac{{\rho_-}^2 d\mu_-}{-d\dot{\lambda}_-} = {\rho_+}^2 D_{\mu+} + {\rho_-}^2 D_{\mu-} \qquad (4.6)$$

p.89: equ. 5.12 $\tau = \mathbf{J}_\mu(\rho)^T \mu$

p.93 equ. 5.17

$$\mathbf{K} \equiv \left(\frac{\partial \tau_i}{\partial q_j}\right) = \left(\frac{\partial (\mathbf{J}^T \mathbf{F})_i}{\partial q_j}\right) = \left(\sum_k \frac{\partial (\mathbf{J}^T)_{ik}}{\partial q_j} F_k\right) + \mathbf{J}^T \left(\frac{\partial F_i}{\partial q_j}\right)$$
$$= \left(\sum_k \frac{\partial (\mathbf{J}^T)_{ik}}{\partial q_j} F_k\right) + \mathbf{J}^T \left(\sum_k \frac{\partial F_i}{\partial x_k} \frac{\partial x_k}{\partial q_j}\right)$$

p.100

$$x' = l_s c_s + l_{se} c_{se} + l_{sew} c_{sew}$$
$$y' = l_s s_s + l_{se} s_{se} + l_{sew} s_{sew} \qquad (5.25)$$
$$s_s = \sin(q_s), \quad s_{se} = \sin(q_s + q_e), \quad s_{sew} = \sin(q_s + q_e + q_w)$$
$$c_s = \cos(q_s), \quad c_{se} = \cos(q_s + q_e), \quad c_{sew} = \cos(q_s + q_e + q_w)$$

As illustrated in figure 5.4B, there are different possible configurations that allow reaching to a given position $(x', y')^T$; that is, this target can be reached with any orientation of the hand permitted by the range of joint motion. For instance, if the task is to grasp a ping-pong ball, then the arm is redundant, as the ball could be grasped with any orientation of the hand. Another example of redundancy is illustrated by the task of pointing with a laser pointer. In this case, the only constraint is that the laser dot be visible at the desired position on the screen, so the arm has excess DOF because this task can be achieved with different orientations of the hand. On the other hand, if the task requires a more specific orientation, as in lifting a mobile phone from a table, the arm is not redundant. Using the model of equation (5.25) for a specific orientation $\theta = q_s + q_e + q_w$ yields

$$x \equiv x' - l_w \cos(\theta) = l_s c_s + l_{se} c_{se}$$
$$y \equiv y' - l_w \sin(\theta) = l_s s_s + l_{se} s_{se} \qquad (5.26)$$

$$\dot{\mathbf{q}}^* = \mathbf{J}^\dagger \dot{\mathbf{x}}, \quad \mathbf{J}^\dagger = \mathbf{J}^T \left(\mathbf{J}\mathbf{J}^T\right)^{-1}, \ \det\left(\mathbf{J}\mathbf{J}^T\right) \neq 0 \qquad (5.30)$$

p.101

p.107

Table 5.2
Anthropometrical data for arm segments used in the simulations

	Mass [kg]	Length [cm]	Center of mass from proximal joint [m]	Mass moment of inertia [kg m^2]
Upper arm	1.93	0.31	0.165	0.0141
Forearm	1.52	0.34	0.19	0.0188
Hand	0.52	0.08	0.055	0.0003

p.113

$$\boldsymbol{\tau}_\mu(\mathbf{q},\dot{\mathbf{q}},\mathbf{u}) = \boldsymbol{\tau}_B(\mathbf{q},\dot{\mathbf{q}},\ddot{\mathbf{q}}) - \mathbf{J}^T\mathbf{F}_E - \Delta\mathbf{F}_E \qquad (6.5)$$

where $\boldsymbol{\tau}_\mu(\mathbf{q},\dot{\mathbf{q}},\mathbf{u}) \equiv \mathbf{J}_\mu^T \boldsymbol{\mu}(\boldsymbol{\lambda},\dot{\boldsymbol{\lambda}},\mathbf{u})$ is the torque vector produced by muscles. In general, muscle viscoelasticity and reflexes make the interaction stable; that is, we can assume that if the perturbation $\Delta\mathbf{F}_E$ is small, $\mathbf{q}$ will remain close to $\mathbf{q}_u$. Therefore, we can use a linear approximation of the restoring force as a function of $\mathbf{e} = \mathbf{q}_u - \mathbf{q}$ in equation (6.5), which gives

$$\boldsymbol{\tau}_\mu(\mathbf{q}_u,\dot{\mathbf{q}}_u,\mathbf{u}) + \mathbf{K}\mathbf{e} + \mathbf{D}\dot{\mathbf{e}} = \boldsymbol{\tau}_\mu(\mathbf{q},\dot{\mathbf{q}},\mathbf{u}) = \boldsymbol{\tau}_T(\mathbf{q}_u,\dot{\mathbf{q}}_u,\ddot{\mathbf{q}}_u) + \Delta\boldsymbol{\tau}_T \qquad (6.6)$$

where $\boldsymbol{\tau}_T(\mathbf{q}_u,\dot{\mathbf{q}}_u,\ddot{\mathbf{q}}_u) \equiv \boldsymbol{\tau}_B(\mathbf{q}_u,\dot{\mathbf{q}}_u,\ddot{\mathbf{q}}_u) - \mathbf{J}^T\mathbf{F}_E$ represents the unperturbed task dynamics and $\Delta\boldsymbol{\tau}_T \equiv \boldsymbol{\tau}_B(\mathbf{q},\dot{\mathbf{q}},\ddot{\mathbf{q}}) - \boldsymbol{\tau}_B(\mathbf{q}_u,\dot{\mathbf{q}}_u,\ddot{\mathbf{q}}_u) - \mathbf{J}^T\Delta\mathbf{F}_E$ the change in the task dynamics due to the

p.117

not vary with speed. Three *phasic synergies* scaled linearly with the movement duration, in a manner similar to equation (6.13), although we would have expected a quadratic relation as muscle activation corresponds roughly to force. D'Avella et al. (2006) were able

p.120

$$\kappa = \frac{0.42}{\sqrt{1+\dot{\mathbf{q}}^T\dot{\mathbf{q}}}} \qquad (6.16)$$

p.148

$$\begin{aligned} z_f^{k+1} &= \vartheta_f z_f^{\,k} + \alpha_f e^k, \quad \vartheta_f, \alpha_f > 0 \\ z_s^{k+1} &= \vartheta_s z_s^{\,k} + \alpha_s e^k, \quad \vartheta_s, \alpha_s > 0 \\ z^{k+1} &= z_f^{k+1} + z_s^{k+1} \end{aligned} \qquad (7.6)$$

where z_f is the output of the fast adaptation process and z_s the output of the slow adaptation process. The total compensation (z) is the sum of the two adaptation processes, each

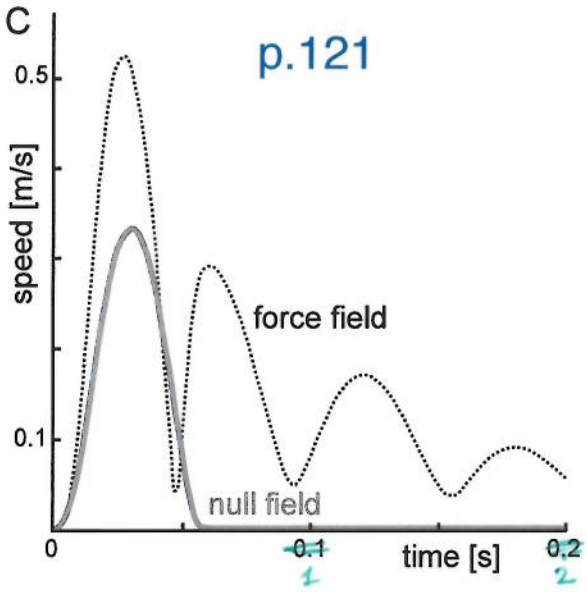

p.121

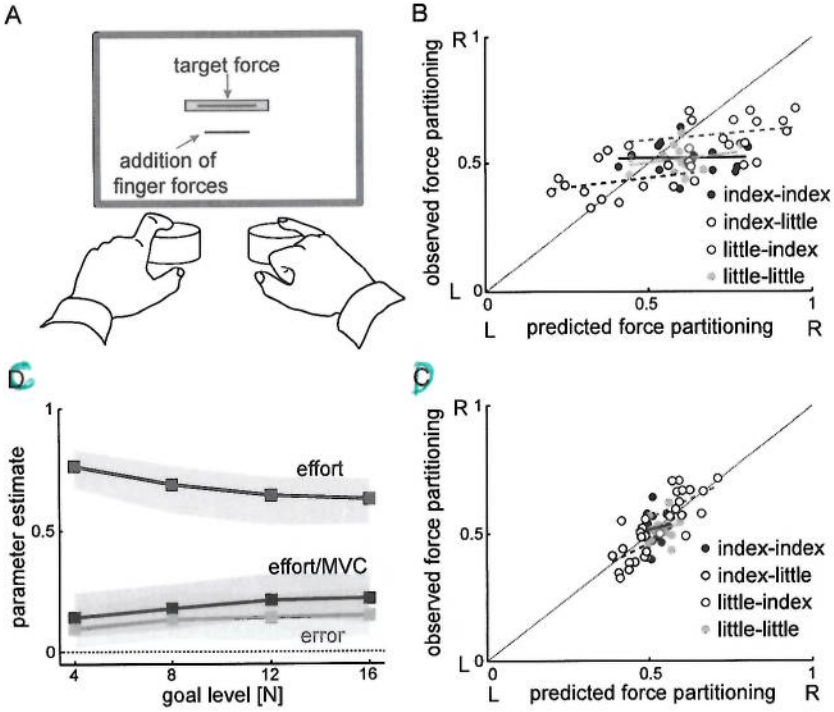

Figure 9.3
Experiment to investigate how two fingers with different noise characteristics share the effort when matching a force target. (A) The experimental setup. (B) and (D) show how the pairs of left and right index/little fingers are used by the subjects if (B) only the deviation is minimized and if (D) effort is also considered. (C) details how error and effort are weighted for the fit shown in (D). Adapted with permission from O'Sullivan, Burdet, and Diedrichsen (2009).

between the fingers, and the third term represents relative effort, normalized by the *maximal voluntary contraction* (MVC).

The parameter values yielding the best fit, shown in figure 9.3C, are plotted in figure 9.3D. These values suggest that although error was considered by the sensorimotor control

$$\mathbf{P}_{(k+1|k)} = \mathbf{A}_k\mathbf{P}_k\mathbf{A}_k{}^T + E[\mathbf{z}_k\mathbf{z}_k{}^T], \mathbf{K}_{k+1} = \mathbf{P}_{(k+1|k)}\mathbf{C}_k{}^T(\mathbf{C}_k\mathbf{P}_{(k+1|k)}\mathbf{C}_k{}^T + E[\mathbf{y}_k\mathbf{y}_k{}^T])^{-1},$$
$$\mathbf{P}_{k+1} = (1-\mathbf{K}_{k+1}\mathbf{C}_k)\mathbf{P}_{(k+1|k)},\ \mathbf{P}_0 = E[\mathbf{z}_0\mathbf{z}_0{}^T] \qquad (9.12)$$
$$\hat{\mathbf{z}}_{k+1} = \mathbf{A}_k\hat{\mathbf{z}}_k + \mathbf{B}_k\mathbf{u}_k + \mathbf{K}_{k+1}(\mathbf{y}_k - \mathbf{C}_k\hat{\mathbf{z}}_k),\ \hat{\mathbf{z}}_0 = E[\mathbf{z}_0]$$

where $E(\mathbf{z}_k\mathbf{z}_k{}^T)$ is the covariance matrix of noise $\boldsymbol{\eta}_k$ and $E(\mathbf{y}_k\mathbf{y}_k{}^T)$ the covariance